Toward a Quantum-Mechanical Description of 2D-IR Spectra of Solvated Systems: The Vibrational Mode Coupling within A Polarizable Continuum Model

Alessandro Biancardi,[†] Chiara Cappelli,*[,†] Benedetta Mennucci,*[,†] and Roberto Cammi*[,‡]

Dipartimento di Chimica e Chimica Industriale, Università di Pisa, Via Risorgimento 35, I-56126 Pisa, Italy, and Dipartimento di Chimica GIAF, Università di Parma, I-43100 Parma, Italy

Received: January 22, 2010; Revised Manuscript Received: March 4, 2010

The extension of the polarizable continuum model (PCM) to evaluate solvent effects on vibrational coupling is reported for both the transition dipole coupling and the Hessian matrix reconstruction (HMR) methods. A comparative analysis of the two approaches is reported for a model system, i.e., formaldehyde dimers in different spatial arrangements, with the aim of dissecting solvent effects in their two main contributions, the modification of the transition dipole moments and the screening of their interaction. The HMR-PCM formalism is finally applied to the evaluation of the vibrational coupling for (*s*)-*N*-methyl acetylproline amide in aqueous and dichloromethane solutions. In the latter case, a comparison with experimental findings is presented and used to gain a better understanding of the conformational state.

1. Introduction

The two-dimensional infrared (2DIR) technique[1−5] is a correlation spectroscopy with similarities to two-dimensional nuclear magnetic resonance (2DNMR). It allows one to follow what happens to the vibrations in a molecule after an initial excitation and provides a two-dimensional spectrum that reveals information on dephasing of the individual vibration and coupling between different vibrations. The latter allows for the determination of structural parameters.

Experimentally, 2DIR spectroscopy has been successfully applied to a wide range of systems. In particular, 2DIR has been shown to be a powerful tool to study polypeptides' structures.[5] These systems, in fact, present structure-sensitive vibrational transitions such as amide-I and amide-II transitions, which, if seen in terms of normal-mode analysis, are mainly carbonyl stretching and in-plane CN−H bending.[6,7] The corresponding 2DIR spectra are, however, very complex to interpret if not supported by a reliable and accurate theoretical method.[1]

A popular approach used to interpret 2DIR spectra is the vibrational exciton Hamiltonian,[8] which assumes that the vibrational modes of interest can be represented by vibrations of local modes, which—to a first approximation—do not interact with the remaining vibrational degrees of freedom of the system. As a result, the exciton model Hamiltonian can be expressed in terms of local-mode basis states. Within this framework, the key ingredients are the vibrational frequencies of each local mode (also called site energies) and their couplings. In turn, the coupling can be modeled with different approaches. One of the simplest methods is the transition dipole coupling (TDC) model,[9−11] which solves the problem in terms of the electrostatic coupling of point dipoles. Because of its simplicity, the TDC model has been extensively used, but there exists many examples proving that the model is not quantitatively reliable.[12] Refinements of the TDC model have been also suggested by including higher-order multipole contributions.[13,14] A more accurate approach, especially when coupled to ab initio methods, is, however, represented by the Hessian matrix reconstruction (HMR) analysis.[15,16] Ab initio geometry optimization and vibrational analysis provide information on eigenvectors, frequencies, and normal-mode transition dipoles. Using the HMR method, one can transform such information into the frequencies of well-defined local modes and intermode vibrational couplings, so that the corresponding exciton Hamiltonian can be constructed.

In order to allow these approaches to reach their full potential, it is of fundamental importance to incorporate solvent effects in all the ingredients of the models. A possible strategy is based on the use of classical molecular dynamics (MD) simulations or hybrid quantum-mechanical/MD approaches, in which the quantum nature of vibrational transitions is retained.[1] As a matter of fact, it appears evident that in many cases the solute−solvent interactions are mainly electrostatic, so that modeling of the solvating environment by a continuum solvation model may provide a good representation of solvent effects on vibrational spectra at a computational cost comparable with that of the corresponding calculation for the isolated system.

Among continuum solvation models, the one developed in our group and known with the acronym polarizable continuum model (PCM) has shown to be a reliable computational tool to study solvated molecular systems,[17] also for vibrational properties and spectroscopies.[18,19] The approach is based on an hybrid quantum-mechanical/classical description where the solvent is represented as a polarizable continuum medium characterized by its macroscopic dielectric properties, whereas the solute, located in a molecule-shaped cavity inside the dielectric, is described at a full QM level. The main advantage of PCM, and the primary reason for its wide application to many problems of chemical interest, is its unique combination of generality and accuracy. In fact, thanks to its most recent formulation (also known as IEF-PCM),[20,21] the model represents a formally exact solution of the electrostatic problem for any kind of charge distribution (i.e., any kind of molecular solute) in several environments of different complexity (not only isotropic and homogeneous solvents but also anisotropic environments, interfaces as well as metal particles of nanoscopic dimension). In addition, PCM presents a very general numerical formulation,

* To whom correspondence should be addressed: E-mail: chiara@dcci.unipi.it; bene@dcci.unipi.it; r.cammi@unipr.it.
[†] Università di Pisa.
[‡] Università di Parma.

10.1021/jp100634p
Published on Web 03/18/2010

which can be extended to many different QM levels still maintaining its important characteristic of allowing for a mutual and self-consistent polarization between the solute charge density and the solvent. This specificity has also permitted to extend the PCM approach to describe environment effects on the electronic energy transfer (EET).[22] By applying this method, we recently discovered that the molecular shape of the donor and acceptor moieties indeed has a strong influence on the screening of their electronic couplings which, for photosynthetic pigments, leads to an exponential attenuation of the screening at separations less than about 20 Å.[23]

In this paper, we present a parallel extension of PCM to describe vibrational energy transfer. Among the different strategies briefly described above, here we shall focus on the TDC and HMR. In both cases, the introduction of the PCM effects requires a revision of both the formalism and the computational algorithms.

The paper is organized as follows. In Section 2, the theory underlying the method and the computational details of the PCM calculations are described. In Section 3, we present and discuss two different applications, namely the PCM-TDC approach to a model system constituted by a formaldehyde dimer in cyclohexane solution and the PCM-HMR model applied to the evaluation of the vibrational coupling for (*s*)-*N*-methyl acetyl-proline amide (NMAP) in water and dichloromethane (DCM) solutions. For the latter, a comparison with experiments will also be reported. Finally, Section 4 reports some conclusive remarks together with a discussion of perspectives on the potentialities of the methods.

2. Methods and Computational Details

As reported in Section 1, the two most commonly used methods for evaluating the vibrational coupling are the TDC and the HMR. Both methods rely on the definition of a set of "local" vibrational modes on the molecular structure, based on some model system, which is chosen depending on the nature of the vibration under investigation.[12,13,16] A key difference between the two methods is that TDC is based on a transition dipole/transition dipole-like interaction, so that only through space interactions are accounted for. On the other hand, HMR is able to account for both through-space and through-bond effects.

In the present work, solvent effects are introduced within the framework of the PCM.[17] In this method, the solute charge distribution in the cavity surrounded by the continuum environment polarizes the dielectric medium, which in turn produces a reaction field acting back on the solute. The solvent reaction field is then introduced in the solute molecular Hamiltonian, and the solution of the Schrödinger equation originates a "new" (polarized) QM charge distribution. This mutual polarization process is continued until self-consistency is reached. In the PCM, the polarization of the solvent is represented by an apparent surface charge density on the boundary of the cavity surface. Over the years, such a formalism has been extended to QM methods to evaluate energy derivatives with respect to many different perturbations. These extensions have made PCM applicable to calculate geometries and properties of various electronic states as well as to study processes and spectroscopies involving both ground and excited states. In the following sections, we shall summarize two new extensions of the PCM approach to describe vibrational couplings among localized vibrations within the HMR and the TDC formalisms.

2.1. HMR-PCM. In the HMR method, the accounting of solvent effects through PCM is obtained by reformulating vibrational frequencies and normal modes for a solvated system, as described before by our group.[19,24] The interested reader can find all the details of the extension of PCM to vibrational properties in the reference papers; here however, it is useful to recall the main aspects of the formalism to make the analysis of the following numerical section easier.

Here we shall mainly focus on the structurally sensitive and strongly IR-active amide-I vibrational mode and, for simplicity's sake, the special case of two interacting amide-I vibrations will be considered. Within the HMR approach, we assume that the amide-I normal modes of the system (Q_1 and Q_2) can be related to two local modes (q_1 and q_2) (the normal modes of a smaller part of the system) by a proper unitary transformation:[16]

$$\begin{pmatrix} Q_1 \\ Q_2 \end{pmatrix} \simeq \mathbf{U}\begin{pmatrix} q_1 \\ q_2 \end{pmatrix} = \begin{pmatrix} \cos\theta & \sin\theta \\ -\sin\theta & \cos\theta \end{pmatrix}\begin{pmatrix} q_1 \\ q_2 \end{pmatrix} \tag{1}$$

By means of the same transformation, both the local-mode vibrational frequencies (or site energies, ε_i) and the intersite coupling β can be obtained, namely:

$$\begin{pmatrix} \varepsilon_1 & \beta \\ \beta & \varepsilon_2 \end{pmatrix} = \mathbf{U}^{-1}\begin{pmatrix} \Omega_1 & 0 \\ 0 & \Omega_2 \end{pmatrix}\mathbf{U} \tag{2}$$

where Ω_i is the vibrational frequency corresponding to the normal mode Q_i. Using the same transformation, the force constant of each local mode, k_i, as well as that corresponding to their coupling, k_{12}, are obtained from the normal-mode force constants. We note that a simple relation exists between the two sets of constants, namely:

$$\beta = \frac{\hbar k_{12}}{2(k_1 k_2)^{1/4}}; \quad \varepsilon_i = \hbar k_i^{1/2} \tag{3}$$

In eqs 1−2, the solvent effects are implicitly accounted for through changes in the geometry of the system (and thus normal modes, Q_i, and vibrational frequencies, Ω_i) as well as through the determination of the local modes q_i. Since amide-I vibrations mainly consist of C═O stretching, the C═O modes of the peptide backbone represent the simplest choice of amide-I local modes. A more accurate description may be obtained by choosing the normal modes of *N*-methylacetamide as local modes of a peptide unit. In both cases, these local modes are recalculated in the presence of the solvent by exploiting the PCM. As a result, both the site energies and the coupling are modified with respect to the isolated system.

2.2. TDC-PCM. Let us start by considering the case of two coupled vibrational modes α and β of two different molecules (represented by their charge distributions ρ_A and ρ_B), hosted in two distinct cavities within a dielectric medium of given dielectric permittivity (from now on denoted as ε). Within the PCM model, each charge distribution ρ_x induces an apparent surface charge polarization σ_x on the boundary of the two cavities.

The force constant, k_{AB}, representing the coupling between the two modes is determined as a mixed derivative of the electrostatic energy of the system (the two charge distributions plus the polarized dielectric medium), V_{AB}^{PCM}, with respect the normal mode coordinates Q_α and Q_β:

$$k_{AB}^{PCM}(Q_\alpha, Q_\beta) = \partial^2 V_{AB}^{PCM}/\partial Q_\alpha \partial Q_\beta \tag{4}$$

In turn, V_{AB}^{PCM} can be written as a sum of different contributions corresponding to the electrostatic interactions: (i) between the bare charge distributions, (ii) between each ρ_x and the apparent surface charge it induces, and (iii) between each ρ_x and the apparent surface charge induced by ρ_y. Due to the symmetry of the kernel of the electrostatic interaction in the case of linear response of the medium, these contributions give rise to two components of k_{AB}^{PCM}, namely:

$$k_{AB}^{direct}(Q_\alpha, Q_\beta) = \int\int \frac{\rho_A^\alpha(\mathbf{r}_i)\rho_B^\beta(\mathbf{r}_j)d\mathbf{r}_i d\mathbf{r}_j}{|\mathbf{r}_i - \mathbf{r}_j|} \quad (5)$$

which is the direct interaction between the two oscillators and

$$k_{AB}^{explicit}(Q_\alpha, Q_\beta) = \int\int_\Sigma \frac{\sigma_A^\alpha(\mathbf{s}_i)\rho_B^\beta(\mathbf{r}_j)d\mathbf{r}_i d\mathbf{s}_j}{|\mathbf{s}_i - \mathbf{r}_j|} \quad (6)$$

which is the explicit contribution due to the polarization of the medium. In eqs 5−7, the upper indexes denote a partial derivative of the corresponding charge distributions with respect to the normal-mode coordinates at equilibrium geometry.

In deriving the equations above, the charge densities of the two oscillators have been assumed as nonoverlapping. Also, the charge density of each unit is independent of the nuclear displacement of the other unit. Such an assumption implies that the cavities have a fixed geometry and do not follow the displacement coordinates of the two oscillators.

If we now assume that the two interacting modes are separated by distances much larger than their size, then a dipolar approximation can be introduced to evaluate the electrostatic interactions, as a result the coupling force constant becomes

$$k_{TDC}^{PCM}(Q_\alpha, Q_\beta) = \boldsymbol{\mu}_A^\alpha \cdot \mathbf{E}_B^{tot} \quad (7)$$

where $\boldsymbol{\mu}_A^\alpha$ is the transition dipole moment of the oscillator α on the unit A and $\mathbf{E}_B^{tot}$ is the total electric field due to the other oscillator plus the contribution due to the polarization of the environment:

$$\mathbf{E}_B^{tot} = \mathbf{E}_B^{\mu_B^\beta} + \mathbf{E}_B^{\sigma_B^\beta} \quad (8)$$

As a result, k_{TDC}^{PCM} becomes the sum of two terms, one due to the *direct* interaction between the two dipoles ($k_{TDC}^{direct} = \mu_A^\alpha \cdot \mathbf{E}_B^{\mu_B^\beta}$) and the other due to the *explicit* polarization effect of the environment. The latter term is determined by the electric field $\mathbf{E}_B^{\sigma_\beta}$ produced by the differentiated charge distribution σ_β, namely:

$$k_{TDC}^{explicit}(Q_\alpha, Q_\beta) = \mu_A^\alpha \cdot \mathbf{E}_B^{\sigma_\beta}(\mathbf{r}) = -\mu_A^\alpha \cdot \nabla \int_\Sigma \frac{\sigma_B^\beta(\mathbf{r}')}{|\mathbf{r} - \mathbf{r}'|}d\mathbf{r}' \quad (9)$$

where ∇ is the gradient operator with respect to the components of the position vector $\mathbf{r}$. In the computational practice, the apparent surface charge distribution is discretized to a set of apparent point charges $\{q_{B,i}^\beta\}$ spread on the cavity:

$$\mathbf{q}_B^\beta = \mathbf{K}\mathbf{V}(\rho_B^\beta) \quad (10)$$

where $\mathbf{q}_B^\beta$ is a column vector collecting the apparent charges. $\mathbf{V}(\rho_B^\beta)$ is a column vector containing the electrostatic potential produced by the molecular charge distribution (ρ_B^β) at the location of the apparent charges, and $\mathbf{K}$ is a square matrix depending on the cavity geometry and the solvent dielectric constant ε.

The molecular quantities involved in the TDC-PCM eqs 7−10 can be determined by performing a QM calculation of normal-mode frequencies and coordinates for the solvated monomers A and B and by extracting the derivatives of the molecular charge density distribution with respect to the normal modes of interest, α and β. For each monomer the PCM calculation of the molecular Hessian is performed using the dimeric cavity, at the corresponding equilibrium geometry. The calculations were performed within the fixed cavity approximation to avoid computational problems in the calculation of the corresponding derivatives of apparent surface charges.

In the derivation of TDC-PCM equations, an equilibrium approach has been implicitly used for the solvent response. As a matter of fact, a nonequilibrium solvation regime can be introduced to take into account effects due to a possible difference between the time scale of the vibrational normal modes of interest and the time scale of the slow component of the solvent response. Such a difference applies to polar solvents, where the slow component corresponds to the molecular reorientation motion, due to the electric dipole moments of the solvent molecules.[25]

We finally note that in the limit of spherical cavities the PCM-TDC formalism can be rewritten in terms of an analytical scaling factor. In this limit, in fact, we can apply the Onsager model and approximate the transition dipoles to a couple of point dipoles at the center of two separated spherical cavities. In this approximation, eq 7 still holds, but now a simple analytical expression for the total electric field $\mathbf{E}_B^{tot}(\mathbf{r})$ can be derived

$$\mathbf{E}_B^{tot}(\mathbf{r}) = \frac{9\varepsilon}{(2\varepsilon + 1)^2}\mathbf{E}_B^{\mu_B^\beta}(\mathbf{r}) \quad (11)$$

As a result, the total force constant reduces to that of two interacting dipoles in gas phase scaled by a screening factor:

$$k_{TDC}^{Ons} = \frac{9\varepsilon}{(2\varepsilon + 1)^2}k_{TDC}^{direct} \quad (12)$$

2.3. Computational Details

All structures were optimized at the DFT level using the B3LYP hybrid functional[26] with the 6-31G(d) basis set for formaldehyde and the 6-311++G(d,p) basis set for NMAP, both in vacuo and solution. Solvent effects were described by exploiting the integral equation formalism (IEF)[20,21] version of PCM,[27] as implemented in the Gaussian03 code (G03).[28] Extension of IEF to the TDC model has been implemented in a locally modified version of the same code.

The PCM molecular cavities surrounding the molecular solutes were built by interlocking spheres. For formaldehyde dimers, the calculations were performed by using for each monomer both a single sphere placed on the carbon atom, with radius $R_{sph} = 3.0$ Å, or a PCM cavity made of four spheres placed on each atom with radii $R_C = 1.925$ Å, $R_O = 1.75$ Å, $R_H = 1.2$ Å. For NMAP the cavity was built by using 13 interlocking spheres with radii $R_C = 1.925$ Å, $R_O = 1.75$ Å, $R_N = 1.83$ Å, $R_{H,\,amide} = 1.2$ Å, $R_{CH} = 2.125$ Å, $R_{CH_2} = 2.325$ Å

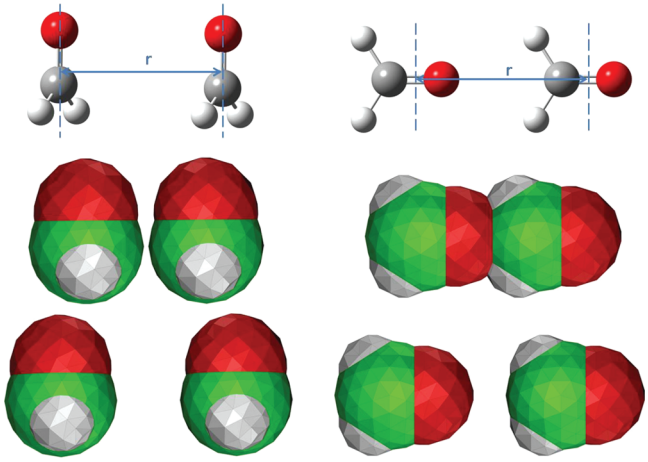

Figure 1. Scheme of the face-to-face (left) and head-to-tail (right) formaldehyde dimers. The corresponding PCM cavities are also shown at 4 and 6 Å distances.

and $R_{CH_3} = 2.525$ Å, according with an analogue choice reported in ref 29. In the following applications, we have analyzed three different solvents, an apolar one for the case of formaldehyde dimer and a medium and a highly polar one for NMAP; the corresponding dielectric constants used are those of cyclohexane ($\varepsilon = 2.0$), DCM, and water ($\varepsilon = 8.9$ and 78.4), respectively.

In the case of NMAP, free energies and Boltzmann populations of the various conformers were obtained by including zero-point and thermal contributions (at 298 K). The same quantities in solvent were obtained by further including nonelectrostatic (repulsion, dispersion, and cavitation) energy contributions.[17]

To apply the HMR approach to NMAP, the amide-I (amide end) and amide-II local modes were represented by the elements of the carbonyl carbon and oxygen atoms and the amino nitrogen and hydrogen atoms in the acetamide ($CH_3-CO-NH_2$) normal modes, whereas the amide-I (acetyl end) local mode was represented by the elements of the carbonyl carbon and oxygen atoms in the *N*-methylacetamide normal modes.

3. Numerical Results

The numerical section is organized as follows. First, in Section 3.1, the TDC-PCM approach is applied to formaldehyde dimers in cyclohexane solution. The results obtained are compared with both TDC in vacuum and the HMR method, where the reconstruction is done by defining vibrational "local" modes on the basis of PCM calculations in solution. In Section 3.2, the HMR method is then further applied to the evaluation of the vibrational coupling of NMAP in water and DCM solutions, for which PCM has proven to be able to give a very good description in the case of other vibrational properties and spectroscopies.[29]

3.1. PCM-TDC vs PCM-HMR: Formaldehyde Dimers. The aim of this section is to show the performance of the PCM-TDC with respect to the more complete HMR method and to benchmark it with respect to the Onsager solvation approach, for which an analytical formulation of the solvent effect on the coupling can be defined (see eq 12). A very simple system formed by two interacting C═O stretching modes placed on two different formaldehyde units is considered. Two different spatial arrangements are considered, i.e., head-to-tail and face-to-face dimers (see Figure 1), both with variable *r* distance between the medium points of the C═O bond.

In Table 1, force constants for head-to-tail and face-to-face formaldehyde dimers in vacuum and in cyclohexane are reported as a function of the *r* distance.

TABLE 1: Coupling Force Constant k_{AB} (10^3 mdyne Å^{-1} amu^{-1}) between the Carbonyl Stretching Modes of the Formaldehyde Dimers[a]

	gas phase		PCM (cyclohexane)	
r	HMR	TDC	HMR	TDC
		Head-to-Tail		
4	2.83	7.30	1.79	7.10(9.24)
6	1.65	2.16	1.31	1.86(2.78)
8	0.79	0.91	0.65	0.77(1.17)
12	0.25	0.27	0.20	0.26(0.35)
16	0.11	0.11	0.08	0.11(0.15)
		Face-to-Face		
4	4.57	3.65	3.83	3.33(4.67)
6	1.12	1.08	0.91	0.94(1.39)
8	0.47	0.46	0.36	0.39(0.59)
12	0.14	0.13	0.10	0.13(0.17)
16	0.06	0.06	0.04	0.05(0.07)

[a] Obtained using HMR and TDC in gas phase and in cyclohexane as a function of the intermolecular distance (*r*, in Å). For the TDC-PCM approach, the *direct* component (see eq 5) is also shown in parentheses.

Looking first at the gas-phase data, it appears that TDC and HMR results are quite different for distances smaller than 12 Å, with TDC overestimating and underestimating the couplings in the head-to-tail and the face-to-fact orientations, respectively. Such a behavior is not unexpected, because the approximation of the two oscillators as a pair of point transition dipoles becomes reasonable only at large distances with respect to the molecular size. Moving to solvated dimers, the analysis becomes more complex as this intrinsic limit of the TDC approach couples with the solvent polarization effect, which acts both on the magnitude of the transition dipoles and on their interaction. From the data reported in Table 1, we can dissect these two effects by comparing the gas phase k_{TDC} with the *direct* component and the total value of the k_{TDC}^{PCM}. As it can be seen from the values of the *direct* component (given in Table 1 in parentheses), the solvent induces a net amplification of the transition dipoles, which would lead to a ca. 30% increase of the dipole−dipole interaction. However, the inclusion of the screening effect completely changes this behavior, leading to a decrease of the total coupling of less than 5% for the head-to-tail and less than 10% for the face-to-face orientation.

In order to get better insight into solvent effects, it is convenient to define a solvent screening factor as

$$s^{PCM} = \frac{k_{AB}^{PCM}}{k_{AB}^{direct}} \tag{13}$$

In Figure 2, we report the distance dependence of *s* for the TDC-PCM in comparison with the screening factor predicted by the Onsager ($s^{Onsager} = 9\varepsilon/(2\varepsilon + 1)^2$) and the Förster[30] approaches ($s^{Forster} = 1/\varepsilon$). For this analysis, two sets of PCM results are reported, the ones obtained from the values reported in Table 1 and the ones obtained in the case of spherical cavities.

As expected, s^{PCM} is a function of the dimer orientation and distance, and it converges to the Onsager factor only at large distances. In the case of spherical cavities, the short-distance discrepancy found for the head-to-tail orientation with respect to the Onsager prediction can easily be explained by noting that at $r = 4$ Å the two spheres slightly overlap and, as a result, the interaction between the transition dipoles is less screened (*s* is

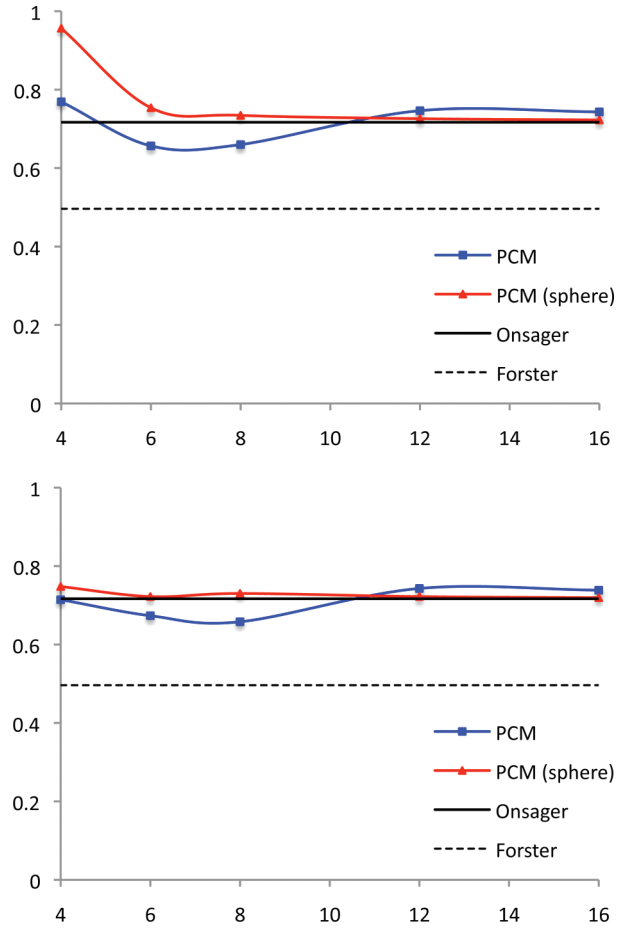

Figure 2. Screening factor (see text) in the formaldehyde dimers as a function of the *r* distance (in Å) for the head-to-tail orientation (upper panel) and the face-to-face orientation (lower panel).

closer to one) than at larger distances, for which the two spheres are separated.

3.2. Vibrational Coupling Between Amide Modes in Peptides: the Case of NMAP. In this section we analyze the vibrational coupling for trans NMAP in aqueous and DCM solutions. The choice of this dipeptide is based on previous studies by some of us,[29] which have shown that PCM is able to give a reliable description of its conformational effects and several spectroscopic properties in water, such as vibrational frequencies, IR/VCD, Raman/VROA, UV/CD spectra, ORD, and NMR.

In order to get a reliable description of spectroscopic properties of systems exhibiting different conformations, not only it is crucial to get an accurate description of the properties but also to correctly predict the relative populations of different conformers. In particular, for NMAP it has been shown,[29] that only 3_{10} helix I and C_7 are stable minima in the gas phase, whereas in water three structures, i.e., 3_{10} helix I, P_{II} and C_7, coexist with different conformational weights. The populations of the most relevant stable conformations calculated in the previous paper for the gas phase and water are reported in Table 2, together with newly obtained values in DCM, whereas in Figure 3, we report the structure of the three possible conformers together with indication of the dihedral angles which identify them.

As reported in the table, results in DCM are in between gas phase and water; in fact, in the gas phase only the C_7 conformation is substantially populated, whereas in water, the P_{II} conformer, unstable in vacuo, is the dominant species, with

TABLE 2: Calculated Boltzmann Populations (%) of the Various Conformers of NMAP in Gas Phase, Water, and DCM

	C_7	3_{10}	P_{II}
gas phase	99	1	–
CH_2Cl_2	17	29	54
water	4	28	68

only a small amount of 3_{10} and an almost negligible quantity of C_7. In DCM an intermediate situation is reported, being P_{II} still prevalent (54%) but with 3_{10} roughly one-half of the P_{II} and C_7, which is no longer negligible (17%).

Such a different picture in the three environments, together with the different values of the coupling of the conformers in each environment, causes quite dissimilar average β values in the various media reported in Table 3 for amide-I−amide-I, Amide−I (Ac)-Amide II, and amide-I (Am)-Amide II. In the same table we also report the corresponding vibrational couplings in vacuo, DCM, and water for the most relevant NMAP conformations. "Ac" and "Am" in the tables refer to the acetyl and amide end, respectively. Due to the near proximity of "vibrational oscillators", only the HMR method has been applied. In fact, for highly interacting chromophores, the dipole−dipole interaction is clearly not reliable as shown also in the previous section, Section 3.1. The use of the HMR method, in fact, makes the resulting couplings account for both through-space and through-bond interactions. The latter should

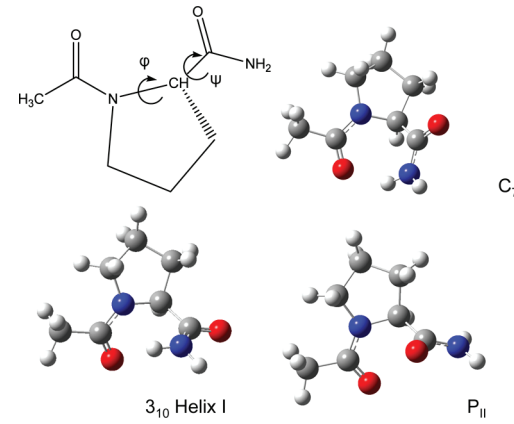

Figure 3. Structures for the three most stable conformers of NMAP.

TABLE 3: Vibrational Couplings (in cm^{-1}) between Amide Modes of NMAP in Gas Phase, Water, and DCM[a]

conformation	gas phase	water	CH_2Cl_2
	Amide-I (Ac) −Amide-I (Am)		
C_7	10.75	9.15	8.23
3_{10}	0.69	2.48	2.24
P_{II}	–	7.00	6.02
average	10.65	5.82	5.28
	Amide-I (Ac)−Amide-II (Am)		
C_7	19.29	17.49	18.14
3_{10}	7.99	11.00	11.14
P_{II}	–	3.11	2.64
average	19.18	5.89	7.79
	Amide-I (Am)−Amide-II (Am)		
C_7	25.85	20.02	20.72
3_{10}	30.43	18.52	21.73
P_{II}	–	18.23	20.67
average	25.89	18.38	20.99

[a] Ac and Am refer to the acetyl and amide end, respectively.

TABLE 4: Angles between Amide Transition Moments[a]

	gas phase	water	CH_2Cl_2
	Amide-I (Ac)−Amide-I (Am)		
C_7	38	30	33
3_{10}	108	116	114
P_{II}	−	70	68
average	39	81	76
	Amide-I (Ac)−Amide-II (Am)		
C_7	33	32	31
3_{10}	71	92	87
P_{II}	−	49	43
average	33	60	54
	Amide-I (Am)−Amide-II (Am)		
C_7	66	55	57
3_{10}	75	60	64
P_{II}	−	66	64
average	66	64	63

[a] NMAP in gas phase, water, and DCM (values in degrees).

TABLE 5: Comparison between Calculated and Experimental Couplings and Angles between Amide Modes of NMAP in DCM[a]

	β	θ
	Amide-I (Ac)−Amide-I (Am)	
calc	5.3	76
exp	9.5 ± 1.5, 10.5 ± 1.5	44 ± 5, 56 ± 5
	Amide-I (Ac)−Amide-II (Am)	
calc	7.8	54
exp	18.6 ± 1.5, 18.8 ± 1.6	35 ± 5, 34 ± 4
	Amide-I (Am)−Amide-II (Am)	
calc	21.0	63
exp	29.6 ± 2, 32 ± 3	52 ± 5, 66 ± 5

[a] β values in cm^{-1} and θ values in degrees. Experimental values are taken from ref 31.

be very large for amide−amide coupling, due to the proximity of the groups involved, in some cases also bonded to each other.

As expected, coupling values are strongly dependent upon the molecular conformation exactly as the angles between transition dipoles (see Table 4), which are, together with β couplings, another outcome of 2DIR experiments.

The 2DIR spectra of NMAP in DCM have been reported by Rubtsov and Hochstrasser,[31] who studied energy transfer pathways between amide modes. In Table 5, a comparison between calculated average data in DCM and experiments is reported.

In general, a good reproduction of experimental findings is shown for both couplings and angles. In more details, couplings are always slightly underestimated with respect to experiments. By analyzing this result together with the data of the single conformers (Table 3), it becomes evident that such an underestimation is a consequence of the underestimation of the population of the C_7 conformer. Exactly the same applies to angles between transition moments. Indeed the study of conformational stability in solvents of low to medium polarity, as DCM, using a continuum solvation model can be more delicate than in highly polar solvents like water. In fact, in DCM, a delicate balance between electrostatic and nonelectrostatic effects applies, which finally leads to free energy differences between the conformers below 0.8 kcal/mol at room temperature. These values are of about the same order of magnitude as the accuracy of the model.

In our opinion, an alternative and more interesting analysis would be to use the calculated couplings of each conformer (see Table 3) to obtain the conformational populations which best fit the experimental β. The result of this fitting is necessarily a range of values, due to the uncertainty in the measured β, but it is centered on populations of 61% for C_7, 28% for P_{II}, and 11% for 3_{10}. This result is in very good agreement with the experimental suggestion of a predominance of C_7, but in the presence of other conformers.[31,32] Indeed, the combination of the experimental couplings with the calculated values of the single conformers can represent an effective strategy to get information on the conformational state of the system, which is difficult to be directly obtained from 2DIR spectra.

4. Summary

We have presented an extension of polarizable continuum model (PCM) to calculate solvent effects on vibrational couplings within the transition dipole coupling (TDC) and Hessian matrix reconstruction (HMR) approaches. In the case of TDC, we have studied a model system with the aim of dissecting solvent effects in their two main contributions, namely the modification of the transition dipole moments and the screening of their interaction. As the two contributions generally act in opposite directions, the final effect can be either an increase or a decrease of the coupling (and as a result a faster or slower energy transfer). The TDC approach, however, cannot be used to get a quantitative description of the phenomenon due to its intrinsic limitations, which remain (and can be further amplified) in the presence of the solvent. As a much more reliable approach, we have presented the HMR-PCM formalism, in which the effects of the solvent are implicitly accounted for by calculating normal modes and frequencies for the solvated system as well as by redefining the local modes in solution.

It is clear that the present study is a preliminary step toward the modeling of 2DIR spectra. However, the application to NMAP shows that the method can indeed be used in combination with experimental measurements to obtain important information on the conformational states of peptides in different environments.

References and Notes

(1) Cho, M. *Chem. Rev.* **2008**, *108*, 1331.
(2) Jeon, J.; Yang, S.; Choi, J.-H.; Cho, M. *Acc. Chem. Res.* **2009**, *42*, 1280.
(3) Ganim, Z.; Chung, H. S.; Smith, A. W.; Deflores, L. P.; Jones, K. C.; Tokmakoff, A. *Acc. Chem. Res.* **2008**, *41*, 432.
(4) Jansen, T. l. C.; Knoester, J. *Acc. Chem. Res.* **2009**, *42*, 1405.
(5) Kim, Y. S.; Hochstrasser, R. M. *J. Phys. Chem. B* **2009**, *113*, 8231.
(6) Schweitzer-Stenner, R. *Vibrational Spectr.* **2006**, *42*, 98.
(7) Barth, A.; Zscherp, C. *Q. Rev. Biophys.* **2002**, *35*, 369.
(8) Mukamel, S. *Principles of Nonlinear Optical Spectroscopy*; Oxford University Press: Oxford, 1995.
(9) Krimm, S.; Abe, Y. *Proc. Natl. Acad. Sci. U.S.A.* **1972**, *69*, 2788.
(10) Torii, H.; Tasumi, M. In *Infrared Spectroscopy of Biomolecules*; Mantsch, H. H., Chapman, D., Eds.; Wiley: New York, 1996.
(11) Torii, H.; Tasumi, M. *J. Chem. Phys.* **1992**, *96*, 3379.
(12) Torii, H.; Tasumi, M. *J. Raman Spectrosc.* **1998**, *29*, 81.
(13) Hamm, P.; Wouterson, S. *Bull. Chem. Soc. Jpn.* **2002**, *75*, 985.
(14) Moran, A.; Mukamel, S. *Proc. Nat. Acad. Sci. U.S.A.* **2004**, *101*, 506.
(15) Ham, S.; Cha, S.; Choi, J.-H.; Cho, M. *J. Chem. Phys.* **2003**, *119*, 1451.
(16) Gorbunov, R. D.; Kosov, D. S.; Stock, G. *J. Chem. Phys.* **2005**, *122*, 224904.
(17) Tomasi, J.; Mennucci, B.; Cammi, R. *Chem. Rev.* **2005**, *105*, 2999.
(18) Tomasi, J.; Cammi, R.; Mennucci, B.; Cappelli, C.; Corni, S. *Phys. Chem. Chem. Phys.* **2002**, *4*, 5697.
(19) Cappelli, C. Continuum Solvation Approaches to Vibrational Properties. In *Continuum Solvation Models in Chemical Physics: Theory and Applications*; Mennucci, B.; Cammi, R., Eds.; Wiley: Chichester, U.K., 2007.
(20) Cancès, E.; Mennucci, B.; Tomasi, J. *J. Chem. Phys.* **1997**, *107*, 3032.

(21) Mennucci, B.; Cancès, E.; Tomasi, J. *J. Phys. Chem. B* **1997**, *101*, 10506.
(22) Iozzi, M.; Mennucci, B.; Tomasi, J.; Cammi, R. *J. Chem. Phys.* **2004**, *120*, 7029.
(23) Scholes, G. D.; Curutchet, C.; Mennucci, B.; Cammi, R.; Tomasi, J. *J. Phys. Chem. B* **2007**, *111*, 6978.
(24) Cammi, R.; Cappelli, C.; Corni, S.; Tomasi, J. *J. Phys. Chem. A* **2000**, *104*, 9874.
(25) Cappelli, C.; Corni, S.; Cammi, R.; Mennucci, B.; Tomasi, J. *J. Chem. Phys.* **2000**, *113*, 11270.
(26) Becke, A. D. *J. Chem. Phys.* **1993**, *98*, 5648.
(27) Miertus, S.; Scrocco, E.; Tomasi, *J. Chem. Phys.* **1981**, *55*, 117.
(28) Frisch, M. J.; Trucks, G. W.; Schlegel, H. B.; Scuseria, G. E.; Robb, M. A.; Cheeseman, J. R.; Montgomery, J. A., Jr.; Vreven, T.; Kudin, K. N.; Burant, J. C.; Millam, J. M.; Iyengar, S. S.; Tomasi, J.; Barone, V.; Mennucci, B.; Cossi, M.; Scalmani, G.; Rega, N.; Petersson, G. A.; Nakatsuji, H.; Hada, M.; Ehara, M.; Toyota, K.; Fukuda, R.; Hasegawa, J.; Ishida, M.; Nakajima, T.; Honda, Y.; Kitao, O.; Nakai, H.; Klene, M.; Li, X.; Knox, J. E.; Hratchian, H. P.; Cross, J. B.; Bakken, V.; Adamo, C.; Jaramillo, J.; Gomperts, R.; Stratmann, R. E.; Yazyev, O.; Austin, A. J.; Cammi, R.; Pomelli, C.; Ochterski, J. W.; Ayala, P. Y.; Morokuma, K.; Voth, G. A.; Salvador, P.; Dannenberg, J. J.; Zakrzewski, V. G.; Dapprich, S.; Daniels, A. D.; Strain, M. C.; Farkas, O.; Malick, D. K.; Rabuck, A. D.; Raghavachari, K.; Foresman, J. B.; Ortiz, J. V.; Cui, Q.; Baboul, A. G.; Clifford, S.; Cioslowski, J.; Stefanov, B. B.; Liu, G.; Liashenko, A.; Piskorz, P.; Komaromi, I.; Martin, R. L.; Fox, D. J.; Keith, T.; Al-Laham, M. A.; Peng, C. Y.; Nanayakkara, A.; Challacombe, M.; Gill, P. M. W.; Johnson, B.; Chen, W.; Wong, M. W.; Gonzalez, C.; Pople, J. A. *Gaussian 03*, revision B.05; Gaussian, Inc., Wallingford, CT, 2004.
(29) Cappelli, C.; Mennucci, B. *J. Phys. Chem. B* **2008**, *112*, 3441.
(30) Forster, T. *Ann. Phys.* **1948**, *2*, 55.
(31) Rubtsov, I. V.; Hochstrasser, R. M. *J. Phys. Chem. B* **2002**, *106*, 9165.
(32) Zanni, M. T.; Gnanakaran, S.; Stenger, J.; Hochstrasser, R. M. *J. Phys. Chem. B* **2001**, *105*, 6520.

JP100634P